Improved Localization and Quantification in Photoacoustic Tomography by Using Acoustic Information Content

Anabela da Silva, Charles Handschin, Christophe Riedinger, Serge Mensah, Hassan Akhouayri

Improved Localization and Quantification in Photoacoustic Tomography by Using Acoustic Information Content

ANABELA DA SILVA[1,*], CHARLES HANDSCHIN[1,2], CHRISTOPHE RIEDINGER[1,2], SERGE MENSAH[3], AND HASSAN AKHOUAYRI[1]

[1] *Aix-Marseille Université, CNRS, Centrale Marseille, Institut Fresnel UMR 7249, 13013 Marseille, France*
[2] *SATT Sud Est (SATT PACA Corse SAS), 8 rue Sainte Barbe, CS 10422, 13205 Marseille Cedex 01, France*
[3] *Aix-Marseille Université, CNRS, Ecole Centrale Marseille, LMA UPR 7051, 13402 Marseille Cedex 20, France*
[*] *Corresponding author: anabela.dasilva@fresnel.fr*

Compiled February 9, 2016

In this letter is proposed a method for improving the localization and the quantification of the optical parameters in photoacoustic tomography of biological tissues, that are intrinsically heterogeneous in both optical and acoustic properties. It is based on the exploitation of both the photoacoustic signal, generated by the heterogeneous optical structures, and the secondary acoustic echoes due to the interaction between a primary photoacoustic wave generated near the tissues surface region and the heterogeneous acoustic structures. These secondary echoes can also be collected through proper measurements of the photoacoustic signals. The experimental procedure is presented as well as the method to filter the signal and the reconstruction algorithm including the account of the acoustic information.

OCIS codes: *(170.5120) Photoacoustic imaging; (170.3880) Medical and biological imaging; (100.3190) Inverse problems.*

http://dx.doi.org/10.1364/ao.XX.XXXXXX

Photoacoustic (PA) tomography is a multiple waves imaging method that seeks primarily at obtaining the optical absorption coefficient of heterogeneously absorbing media, by resolution of an inverse problem. Biological tissues are both heterogeneously optically absorbing and diffusing media. The accurate quantification of the optical absorption coefficient is obtained provided the optical diffusion process is accounted for [1]. Multiple sources illumination [2, 3] is a method to discriminate optical absorption and diffusion: the medium is actively probed, locally, under various incidences, to assess its response.

Another advantage, not exploited so far, of performing local illumination is that it generates near the interface a photoacoustic wave. Usually, this signal is (time) filtered or not measured (transducers oriented in specific directions). However, this PA wave, originating from the external boarder of the object (we call it the Boarder PA (BPA) wave), generally follows a longer ray path within the object. Therefore, it is more likely to be scattered by any of the acoustical heterogeneities than PA waves, induced by internal optical heterogeneities. In addition, knowing the exact position of the BPA source makes it possible to perform diffraction measurements that lead to the separation of the scattered field from the incident field. While the incident field is representative of the BPA source (power, directivity) and gives information about the mean speed of sound along the ray path, the scattered field carries information on the acoustical heterogeneities (localization, geometry and impedance contrast). Besides, the pressure amplitude of the BPA wave can be eventually increased by considering an optically absorbing coating of the external boarder of the object probed. Thus, with local sources illumination, the interesting point is that two different echoes sequences coexist that can be separated in respect with the physical processes from which they originate. The two waves (BPA and PA) can be exploited separately. Indeed, with BPA, both the time of generation and the localization of the BPA point source can be used as prior knowledge. As a consequence, the BPA wave brings spatial information that can be introduced afterwards in the PA signal processing to retrieve the optical properties.

In this letter, we want to take advantage of the pure acoustic information contained in the photoacoustic measured signal. First the phenomenon is described through examples of measurements performed on tissue-mimicking phantoms, showing the feasibility of such measurements. The information content of the acquired signals is presented and dicussed. The signal processing protocol is detailed and the motivation of using the acoustic echoes measurements as prior knowledge is illustrated through reconstructions performed on synthetic phantoms.

The principle of photoacoustic probing consists in heating the medium with a time varying optical source and collecting the acoustic waves generated by thermal expansion with conventional acoustic detectors (transducers). In our setup (Fig. 1(a)), a pulsed laser (Quantel, France, Nd:Yag, 1064 nm, 330 mJ, 5 ns, 10 Hz, frequency doubled by a KTP crystal at 532 nm) and immersion acoustic transducers (diameter 10 mm, focal length 1”,

central frequency 3.5 MHz, Olympus, France) are used. The illumination beam was enlarged in the transverse direction (beam diameter on the surface of the object 40 mm). The collected signal is then preamplified (preamplifier Olympus, France, gain 40 dB, cutting frequency 10 MHz) and drived to an oscilloscope (Tektronix, USA, 4 channels, bandpass width 200 MHz) for signal analyzis. Sound and light velocities being so different, the optical fluence can be supposed to be deposited instantaneously within the whole medium according to the spatial distribution of the absorption and the diffusion coefficients. The deposited energy is dissipated into heat, microdilatations are produced that give birth to pressure waves that propagate and sense the medium.

If the medium is homogeneous in terms of both optical and acoustic properties, a single acoustic pressure wave echo, is going to be measured due to the deposition of energy, mostly near the illuminated surface because of the short scattering mean free path (few μm in biological tissues). Hence its time-of-flight corresponds mostly to the distance between the illuminated surface and the detector position. This initial pressure wave, i.e. the BPA wave, propagates and potentially probes the medium as a conventional acoustic wave (Fig. 1(a), wave in green).

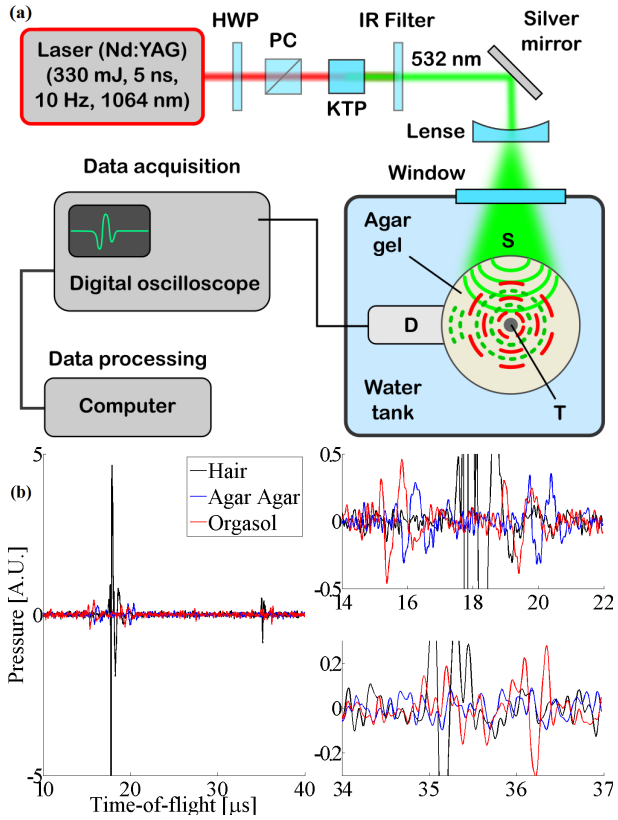

Fig. 1. (a): Schema describing the different types of echoes that can be measured; (b): Left, example of measurement on an agar-agar based phantom with different inclusions in its center; Right, zoom on the photoacoustic (top) and the acoustic echoes (bottom) generated by the inclusions

If acoustic heterogeneities are present in the medium, for example because of a different density as in tumors (mammary tumors are visible with US echography), then this BPA wave is going to be perturbed, and echoes related to the presence of acoustic heterogenities will be sensed at longer times-of-flight. If optically absorbing heterogeneities are present within the medium, more energy will be absorbed locally giving birth to the conventional photoacoustic echoes (Fig. 1(a), wave in red) arriving at a shorter times-of-flight compared to the above mentioned photoacoustic echo generated at the interface.

To illustrate this purpose, a series of demonstrating experiments were conducted under the experimental configuration described in Fig. 1(a): cylindrical phantoms (∅=5 cm) were made of a aqueous gels of a mixture of agar-agar (wt2%, Jeulin, France) and titanium dioxyde (TiO_2) powder (wt0.05%, Sigma-Aldrich, France) to mimick the level of optical scattering of the tissues (estimated reduced scattering coefficient 6 cm^{-1}, and absorption coefficient 0.02 cm^{-1} at 532 nm), in the center of which were introduced inclusions of different nature: i) a thin black hair, typical example of dual heterogeneity (high absorption, high density); ii) a cylindrical absorbing inclusion (∅=0.6 cm) made of the same mixture of agar-agar/TiO_2 to match the acoustic properties of the background, to which a small amount of black India ink (Pelikan 17, Germany) was added (measured absorption coefficient 0.4 cm^{-1} at 532 nm); a cylindrical inclusion (∅=0.6 cm) containing the same mixture of water/agar-agar/TiO_2 to which was added a wt30% of orgasol (Orgasol 2001 EXD NAT1, Arkema, France) that modifies essentially the speed of sound (estimated speed of sound $\sim$ 1700 $m.s^{-1}$) and not much the density (1.03 $g.cm^{-3}$ for Orgasol wt100%) [4]. Measurements collected on transducer D, perpendicular to the illumination path, are reported on Fig. 1. As the three inclusions are placed at the same position (center of the cylinder), the photoacoustic echoes arrive approximately at the same time-of-flight $t_{id} \sim 18$ μs (see zoom, Fig. 1 (b), right,top), corresponding to the distance inclusion-detector. In the pressure measurements of the two phantoms containing acoustic heterogeneities (hair, black line, and orgasol, red line), it can be orbserved the presence of a second echoe (see zoom, Fig. 1 (b), right,bottom), arriving at a time-of-flight corresponding to the path source-inclusion-detector: $t_{si} + t_{id} \sim$ 35-36 μs. The phantom containing a purely optical hetrogeneity (Agar-agar with ink inclusion) does not exhibit any acoustic echo on Fig. 1 (b) (blue line).

Hence, exploiting these secondary acoustic echoes due to the presence of burried structures that are inhomogeneous both acoustically and optically, as it is the case of tumors, offers the possibility to retrieve spatial information on the location and/or on the acoustic properties of the medium (sound speed). This information can afterwards be included in the reconstruction of the optical parameters as priors, in order to, alternativelly, speed up the reconstructions or improve their qualities. The main difficulty lies in sorting temporally signals of different nature. One has to clearly discriminate the two species of waves, the PA ones from the scattered BPA ones. By the way, the corresponding species of echoes belong to two different time spaces delimited by the position of the interface, localized in this measurement at $\sim$ 24 μs: (i) photoacoustic echo localizes an object T belonging to a circle $\mathscr{C}$ of radius $\overline{TD} = t_{id}/v_s$, v_s being the sound velocity; (ii) acoustic echo localizes an object T belonging to an ellipse $\mathscr{E}$ of foci the position of the detector D and the projection of the laser beam at the surface of the phantom such that $\overline{ST} + \overline{TD} = (t_{si} + t_{id})/v_s$. Hence, the object T belongs to the intersection of $\mathscr{C}$ and $\mathscr{E}$ that occurs inside the phantom area. For multiple objects localization, one has to multiply the measurements and plot all possible occurences.

Hereafter we explain, through a 2D simulation example, how the measures of these secondary signals can be exploited and introduced in a reconstruction algorithm to reconstruct

the optical parameters. The simulations were done on a homogeneous disk phantom containing five inhomogeneous regions. The maps of the values of the physical parameters are reported on Fig. 2, 1st row. Synthetic pressure measurements are simulated by first computing the initial pressure distribution $p_o(\mathbf{r}) = \Gamma(\mathbf{r})\mu_a(\mathbf{r})\phi(\mathbf{r})$, Γ [-] being the Grüneisen coefficient, μ_a [cm^{-1}] the optical absorption coefficient, ϕ [W.cm^{-2}] the fluence, and $\mu_a\phi$ [W.cm^{-3}] is the absorbed power density (specific optical absorption) transformed into heat at position $\mathbf{r}$. As the medium fulfills the Diffusion Approximation assumptions [5] (large medium, scattering predomining on absorption), $\phi(\mathbf{r})$ can be determined by solving the Diffusion Equation (numerically, with the Finite Element Method in the present case), in the Continuous Wave (CW) regime: $\mu_a\phi_s - \nabla\cdot(D\nabla\phi_s) = S_s$, with optical source S_s located at points belonging to the periphery of the organ, and D the diffusion coefficient [cm]. Robin boundary conditions apply at the diffusing/non-diffusing boundary between the organ and the outside space. Equations of linear acoustics can be used to model the time evolution of photoacoustic wave fields (isotropic media, irrotational pressure flow, shear waves neglected) [6]: $\frac{\partial \mathbf{u}}{\partial t} = -\frac{1}{\rho_0}\nabla p$; $\frac{\partial \rho}{\partial t} = -\rho_0\nabla\cdot\mathbf{u}$; $p = v_s^2\rho$; where the initial conditions are given by: $p(\mathbf{r}, t=0) = p_0(\mathbf{r})$; $\frac{\partial p(\mathbf{r},t=0)}{\partial t} = 0$. The k-wave toolbox was used to solve the acoustic propagation [7]. In the present example, 360 transducers were evenly distributed at the periphery of the object and a set of 8 different point sources experiments, also evenly distributed, were run. The final sinogram was composed of 8×360 time-resolved measurements, an example is plotted on Fig. 2, 2^{nd} row 1^{st} column, showing the complexity of the signals. From the sinograms, an algorithm of peak detections is applied [8], and the spatial histogram of probabilities of intersections between circle $\mathscr{C}$ and $\mathscr{E}$ is calculated. The gradient of the resulting image (Fig. 2, 2^{nd} row 2^{nd} column) is taken to obtained enhanced contours and a final thresholding allows the identification of a limited number of regions of interest, representing the most favorable regions of location of tumors (Fig. 2, 2^{nd} row 3^{rd} column). Reconstructions of the unknown physical parameters can then be spatially focused to these regions of interest.

A minimization based approach has been adopted for the resolution of the inverse problem, in which it is sought to find $(\mu_a(\mathbf{r}), D(\mathbf{r}))$ which minimizes the error functional $F = \frac{1}{2}\sum_s \int_\Omega (p_s^m(\mathbf{r}) - p_s(\mathbf{r}, \mu_a(\mathbf{r}), D(\mathbf{r})))^2 d\mathbf{r}$, where p_s^m is the measured initial pressure distribution map due to source s, that can be obtained from the measured pressures, after resolution of the acoustic propagation inverse problem. Here, to test the feasibility, we considered an ideal initial pressure distribution map $p_s^m = \Gamma\mu_a\phi_s$, obtained from the multiplication of the Grueneisen coefficient Γ (kept constant, here), the absorption coefficient distribution map and the fluence deposited by source s calculated by solving the diffusion equation. The reconstructions of the optical parameters have been performed with an adjoint-assisted gradient-based method with Total Variation (TV, regularization parameter 0.1) constraint on parameter μ_a [9, 10]. The reconstructions obtained with and without use of the localization map are shown on Fig. 2 (two last rows). As expected and as it can be seen on the error plots, the reconstructions of the absorption and diffusion coefficients are improved by using a priori knowledge on the positionning of the heterogeneities. Moreover, the reconstructions are obtained with a much faster computation time, as the number of unknows is reduced with localized reconstructions.

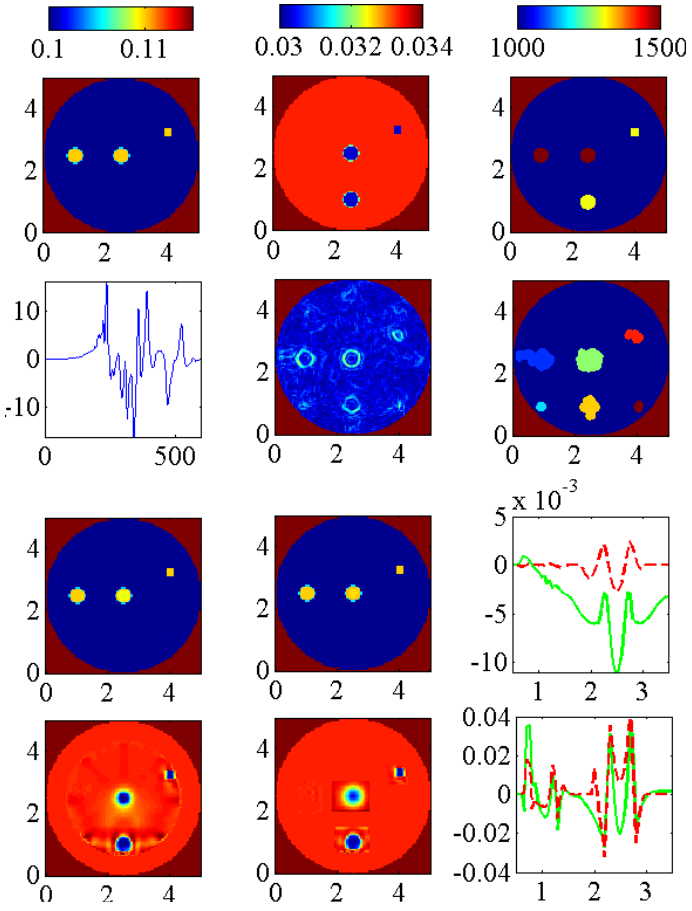

Fig. 2. Inverse problem resolution. 1^{st} row: map of the spatial distribution of the absorption coefficient μ_a [cm^{-1}], diffusion coefficient D [cm] and speed of sound v_s [m.s^{-1}]. 2^{nd} row: example of measurement [a.u.], gradient image of the probability of presence of inhomogeneities, thresholded map. 3^{nd} row: Reconstruction without prior knowledge of μ_a only (left) and μ_a simultaneously with D (center), error along the horizontal direction, at height 2.5 cm (green line: μ_a only; red line μ_a and D. 4^{th} row: Reconstruction of D without (left) and with (center) prior knowledge, error along the vertical direction, at width 2.5 cm, without (green line) and with (red line) prior knowledge.

In conclusion, the method proposed for the registration and processing of the photoacoustic measurements allows more accurate reconstructions with efficient computation times. The method relies in sorting the different sources of echoes, which is made feasible as primary PA and secondary BPA echoes are clearly identified in time. Moreover, the method can be improved by exploiting more quantitatively the BPA echoes by using proper acoustic model-based reconstuction algorithms [11]. The measurement of these echoes may also be facilitated by using a time-gated amplification.

FUNDING INFORMATION

Funding. Agence National pour la Recherche (ANR) (AVENTURES-ANR-12-BLANBS01-0001-04); SATT-SE programme de maturation Mammoscan.

REFERENCES

1. A. Rosenthal, D. Razansky, and V. Ntziachristos, "Quantitative optoacoustic signal extraction using sparse signal representation," Medical Imaging, IEEE Transactions on **28**, 1997–2006 (2009).
2. G. Bal and K. Ren, "Multi-source quantitative photoacoustic tomography in a diffusive regime," Inverse Problems **27**, 20p (2011).
3. N. Song, C. Deumié, and A. Da Silva, "Considering sources and detectors distributions for quantitative PhotoAcoustic tomography (QPAT)," **5**, 3960–3974.
4. E. Franceschini and R. Guillermin, "Experimental assessment of four ultrasound scattering models for characterizing concentrated tissue-mimicking phantoms," The Journal of the Acoustical Society of America **132** (2012).
5. T. Vo-Dinh, *Biomedical Photonics Handbook* (CRC Press, 2003).
6. P. Morse and K. Ingard, *Theoretical acoustics* (Harwood Academic, 1991).
7. B. T. Cox, S. Kara, S. R. Arridge, and P. C. Beard, "k-space propagation models for acoustically heterogeneous media: Application to biomedical photoacoustics," Journal of the Acoustical Society of America **121**, 3453–3464 (2007). 6.
8. N. C. Yoder, "Matlab function 'peakfinder.m'," // http://www.mathworks.com/matlabcentral/fileexchange/25500-peakfinder-x0--sel--thresh--extrema--includeendpoints--interpolate-. (Copyright (c) 2015).
9. B. C. Paul C. Beard, Jan G. Laufer and S. R. Arridge, "Quantitative photoacoustic imaging: Measurement of absolute chromophore concentrations for physiological and molecular imaging," in "Photoacoustic Imaging and Spectroscopy," , L. V. Wang, ed. (CRC Press, 2009).
10. H. Gao, H. Zhao, and S. Osher, "Bregman methods in quantitative photoacoustic tomography," University of California Los Angeles (UCLA) Computational and Applied Mathematics Reports **Vol. 10 – 42** (2010).
11. S. Mensah and E. Franceschini, "Near-field ultrasound tomography," The Journal of the Acoustical Society of America **121** (2007).